Study of Partial Discharge Based on Time-Frequency Analysis Using Local Polynomial Fourier Transform

Estudio de Descargas Parciales Basado en un Análisis Tiempo-Frecuencia Usando la Transformación Local Polinomial

María C. Forero[1], Herbert E. Rojas[2]

ABSTRACT

In recent years, for partial discharge (PD) analysis, signal processing techniques have been applied in the time-frequency domain such as Short Time Fourier Transform (STFT), Wavelet Transform (WT) and Wigner Distribution (WD), among others. Local Polynomial Fourier Transform (LPFT) is a linear time-frequency representation which is a generalization of STFT. This paper present a study of partial discharge based on time-frequency analysis using Local Polynomial Fourier Transform. The analyzed PD signals were simulated using two mathematical models: PD single-pulse model and PD pulse sequence model. As part of the study, the waveform of PD signals selected were characterize in the time domain and the Fast Fourier Transform (FFT) was used in the analysis at frequency domain. Finally, to demonstrate the versatility of the proposed signal processing technique (based on LPFT) and its application on PD signals, the results obtained with the LPFT of polinomial order m=2 and m=3 were compared with those obtained applying STFT. The results show that the LPFT is able to reveal low and medium frequency components which are due to the secondary peaks and oscillations of the PD pulses, which are not detected when the STFT is used.

Keywords: instantaneous frequency (IF), local polynomial Fourier transform (LPFT), partial discharges (PD), time-frequency analysis,

RESUMEN

Durante los últimos años, para el análisis de descargas parciales (DP) se han venido usando técnicas para el procesamiento de señales en el dominio tiempo-frecuencia como la transformación de corto tiempo de Fourier (STFT), la transformación de Wavelet (WT) y la distribución Wigner (WD), entre otras. La transformación local polinomial de Fourier (LPFT) es una representación tiempo-frecuencia lineal que generaliza la STFT. Este trabajo presenta un estudio relacionado con la aplicación de la LPFT para el análisis y caracterización de señales generadas por DP. Las señales de DP analizadas son generadas a partir de simulaciones que aplican un modelo matemático para producir pulsos sencillos y secuencias de pulsos. Como parte del estudio, sobre las señales de DP seleccionadas se realizó un análisis en el dominio del tiempo para caracterizar las formas de onda y se usó la transformada rápida de Fourier (FFT) para hacer un análisis en el dominio de la frecuencia. Finalmente, para demostrar la versatilidad de la técnica de procesamiento propuesta (basada en la LPFT) y su aplicación en señales de DP, se comparan los resultados obtenidos usando LPFT de orden polinomial m=2, m=3 y una técnica convencional como es la STFT. Los resultados muestran que la LPFT es capaz de revelar componentes de baja y media frecuencia que se relacionan con los picos secundarios y las oscilaciones de los pulsos de DP, los cuales no son detectados cuando se usa la STFT.

Palabras clave: análisis tiempo-frecuencia, descargas parciales (PD), frecuencia instantánea (IF), transformación local polinomial de Fourier (LPFT)

Received: July 17th 2015
Accepted: Oct 15th 2015

Introduction

Traditionally, the analysis methods for signal processing of discharge (PD) are based on the time or frequency domain. In the case of the time domain, some features of the signal, such as time intervals, amplitude levels are easily extracted for visual inspection but are susceptive to noise (Sejdić, Djurović, & Jiang, 2009). Otherwise, in the frequency domain techniques as the Fourier transform (FT) can get the amplitude spectrum and the power spectrum of signals, however it cannot get the information in time-frequency plane. Further, the FT assumes the stationarity of the signal (Katkovnik, 1995), which in the analysis of PD is not satisfied because they are non-periodic signals and the fast transient features in the PD signals can be ignored o cannot be revealed efficiently Ma, Zhou, & Kemp, 2002). For these reasons, the FT has serious limitations as analysis method of PD.

In last decades, several researchers have used time-frequency (TF) analysis methods to study the electromagnetic disturbances, which are non-stationary signals as the PD. Some examples of

[1] María C. Forero. Electrical Engineering Student, Universidad Distrital Francisco José de Caldas, Colombia. Electromagnetic Compatibility and Interference Group GCEM, Colombia. Correspondence author, E-mail: mcforerom@udistrital.edu.co. Tel: +57-1-7051800 Ext: 2128

[2] Herbert E. Rojas. Electrical Engineer, M.Sc. in Electrical Engineering and candidate to Ph.D. from Universidad Nacional de Colombia, Colombia. Assistant Professor in Electrical Engineering Department, Universidad Distrital Francisco José de Caldas Colombia. Electromagnetic Compatibility and Interference Group GCEM. E-mail: herojasc@udistrital.edu.co

these signal-processing techniques are the short-time Fourier transform (STFT), the Wigner-Ville distribution (WVD), the Wavelet transform (WT), the fractional Fourier transform (FRFT) and the local polynomial Fourier transform (LPFT). These techniques provides information of amplitude levels in TF bands and the energy concentration of the signal, i.e they provides time and frequency characteristics at the same time (Li, Bi, Stankovic, & Zoubir, 2011).

With respect to the study of PD, the STFT has been used to identification of PD from acoustic emission signals (Chai, Md Thayoob, Ghosh, Sha'ameri, & Talib, 2006), In (Lu & Boxue, 2008)(Lu & Boxue, 2008) to study PD in transformers a pattern recognition method using filtering in time-frequency domain is presented. Other signal processing techniques used in the analysis of PD are the Wavelet Transform (WT) and Wigner Distribution (WD). (Ma, Zhou, & Kemp, 2002; Phukan & Karmakar, 2000) and (Caironi et al., 2002) some example of PD study use WT and WD.

The LPFT is a generalization of the STFT which provides better energy concentration and higher resolution using a polynomial in its complex exponent (Sejdić et al., 2009). Additionally, the LPFT can be used to estimate the instantaneous frequency (IF) of a signal and its derivatives (Li et al., 2011). These elements allow the LPFT to determine approximately the time-frequency variations of a signal.

LPFT has been used in several applications such as signal processing of varying signals, singularity detection, radar imaging (Popović, Djurović, Stanković, Thayaparan, & Daković, 2010); (Sun, Wang, Fang, Yang, & Song, 2015), (Thayaparan, Djurovic, & Stankovic, 2006), interference suppression in communications (Stanković & Djukanović, 2005) sonar and the IF estimation (Katkovnik, 1995). However, LPFT has not been used to analysis of electromagnetic interference as the PD. This paper presents an analysis of PD signals using the LPFT. These signals were simulated applying the mathematical model proposed by (Mortazavi & Shahrtash, 2008)-

The rest of this paper is organized as follows: the mathematical structure of STFT and LPFT is described in Section 2. The parameters and model of PD pulses used in simulations are presented in Section 3. In Section 4, the analysis in time domain and frequency domain of PD signals is presented. The time-frequency analysis of PD single-pulse and PD pulse-train using LPFT is described in Section 5. Finally, conclusions are drawn in Section 6.

Theory of time–frequency analysis

Short–time Fourier Transform (STFT)

The STFT is evaluated by applying a suitable windowing function to the original signal and evaluating the conventional Fourier transform (FT) of the resulting length sequence (Katkovnik, 1995). The STFT of the signal $y(t)$ is expressed as follows:

$$Y_h(\omega,t)=\int_{-\infty}^{\infty}\rho_h(u)y(t+u)e^{-j(\omega u)}du \qquad (1)$$

Where ρ_h is a windowing function and h is a length of the window. The spectral content at the point t, defined as periodogram, can be given by:

$$I_h(\omega,t)=|Y_h(\omega,t)|^2 \qquad (2)$$

STFT is simple to implement but it provides low resolution for time-varying signals (Li et al., 2011).

Local polynomial Fourier Transform (LPFT)

LPFT is a generalized form of the STFT and it is a linear time-frequency representation (L-TFR), which is defined as (Katkovnic, 1995):

$$Y_h(\bar{\omega},t)=\int_{-\infty}^{\infty}\rho_h(u)y(t+u)e^{-j\theta(u,\bar{\omega})}du \qquad (3)$$

To calculate the LPFT computationally, it is better to use the following definition:

$$Y_h(\bar{\omega},t)=\sum_{n=-\infty}^{\infty}\rho_h(nT_s)y(t+nT_s)e^{-j\theta(u,\bar{\omega})} \qquad (4)$$

Where y is the signal, T_s is the sampling time of the signal. The function $\rho_h(nT_s)$ is windowing function of length of the window h that formalizes the location of fitting with respect to the center point nT_s. The function ρ_h is a finite support function and must satisfy the following properties used in non-parametric estimation, in particular:

$$\begin{aligned}&\rho_h(u)\geq 0,\quad \rho(0)=\max_u\rho_h(u)\\ &\rho_h(u)\to 0\ \text{ as }\ |u|\to\infty\quad;\quad \int_{-\infty}^{\infty}\rho_h(u)du=1\end{aligned} \qquad (5)$$

Where $u=nT_s$. In (4) the exponential term $\exp[-j\theta(u,\bar{\omega})]$ is the LPFT kernel function defined as:

$$\theta(u,\bar{\omega})=\omega_1 u+\omega_2\frac{u^2}{2}+\cdots+\omega_m\frac{u^m}{m!} \qquad (6)$$

The set of LPFT estimators for IF (first-order) and higher orders is defined as $\bar{\omega}(t)=\big(\omega_1(t),\omega_2(t),\omega_3(t),\dots,\omega_m(t)\big)$, where $\bar{\omega}\in R^m$ and m is the LPFT polynomial order. From the definition shown in (3), it can be concluded that $Y_h(\bar{\omega},t)$ is a periodic function of $\bar{\omega}\in R^m$, with periods equal to $2\pi\, s!/T^s$ with $s=1,2,\dots,m$.

Similarly, to the STFT periodogram (2), which is defined as an energy distribution in the conventional time-frequency plane $t-\omega(t)$, the Local polynomial periodogram (LPP) is defined as an energy distribution in the $t-\bar{\omega}(t)$ space, as follows:

$$I_h(\bar{\omega},t)=|Y_h(\bar{\omega},t)|^2 \qquad (7)$$

The LPP allows to determine the energy concentration distribution and estimate the IF of a signal (Katkovnik, 1997; Li & Bi, 2009). When, $m=1$ the LPFT $Y_h(\bar{\omega},t)$ in (4) becomes to the STFT defined in (1) and $I_h(\bar{\omega},t)$ in (7) becomes to the conventional periodogram presented in (2). However, when m increases, the complexity of the polynomial exponent in (6) also increase. Therefore, the LPFT could be interpreted as an L-TFR that shows an energy distribution in $t-\bar{\omega}(t)$ space with the highest level of detail.

To determine the values of $\bar{\omega}(t)$ at each time, the LPA looks for the highest energy concentration points in the LPP defined in (8), by the following optimization problem (Katkovnik, 1997):

$$\bar{\omega}(t,h)=\underset{\bar{\omega}\,\epsilon\, Q\,\subset\, R^m}{arg\max} I_h(\bar{\omega},t) \qquad (8)$$

The adequate location of the estimators from the LPA is insured through the window function ρ_h. This function only considers the observations in the neighborhood of a "center" point t. There are different ways to solve the optimization problem described in (8).

Simulation parameters

PD single-pulse model

For study and computation of PD signals, single-pulses were mathematically defined for the analysis in time and frequency domain. In this case, the model used in the simulation of PD pulses was a damping oscillatory exponential function defined as follows (Mortazavi & Shahrtash, 2008):

$$x(t) = \begin{cases} Ae^{-(t-t_0)/\tau}\cos(2\pi f_0(t-t_0)) & t \geq t_0 \\ 0 & t < t_0 \end{cases} \quad (9)$$

Where, A is the amplitude of the pulse, t_0 is the time of pulse occurrence, τ is the damping factor and f_0 is the frequency of oscillation. An example of a PD single-pulse signal is shown in Figure 1.

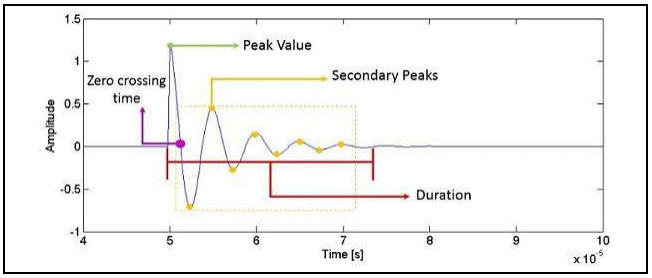

Figure 1. PD single-pulse signal
Source: authors

The characteristics of the PD pulse waveform are defined as:

- Peak value: maximum value of the PD pulse
- Secondary peaks: quantity of positive or negative peaks with amplitudes between the peak value and above 2% of the peak value
- Duration: time period when PD pulse occurs
- Zero crossing time: first point where the signal changes from positive to negative (or vice versa) and the signal value is zero

PD pulse sequence model

Experimental applications provide measurements of sequential PD with different characteristics. In this paper, the pulse sequence (PS) is defined as a pulse train signal consisted by three successive PD single-pulses. This model is given by:

$$x(t) = \begin{cases} A_0 e^{-\frac{t-t_0}{\tau}}\cos(2\pi f_0(t-t_0)) & t \geq t_0 \\ 0 & t < t_0 \\ A_1 e^{-\frac{t-t_1}{\tau_1}}\cos(2\pi f_1(t-t_1)) & t \geq t_1 \\ 0 & t < t_1 \\ A_2 e^{-\frac{t-t_2}{\tau}}\cos(2\pi f_2(t-t_2)) & t \geq t_2 \\ 0 & t < t_2 \end{cases} \quad (10)$$

Where, A_i is the amplitude, t_i is the occurrence time, τ_i is the damping factor and f_i is the oscillation frequency of each single-pulse i that composes the PD sequence pulse. The characteristics of the PD waveform with three pulses is like as the model of one pulse. In this paper, three signals are selected as case studies: two PD single-pulse (PD1 and PD2) and one PD pulse train (PD3). Table 1 shows the variables used in simulations to obtain the PD pulses using (9) and (10). In addition, Figure 2 shows the waveform of PD1, PD2 and PD3 signals.

Table 1 Variables of simulate PD

Variable / Signal	*PD1*	*PD2*	*PD3*
$A\ [p.u.]$	0.8	1.2	$A_1 = 0.8; A_2 = 1.0; A_3 = 1.2$
$t\ [\mu s]$	50	150	$t_1 = 50; t_2 = 150; t_3 = 275$
$\tau\ [\mu s]$	3	7	$\tau_1 = 3; \tau_2 = 3; \tau_3 = 3$
$f\ [KHz]$	300	300	$f_1 = 150; f_2 = 300; f_3 = 260$

Source: authors

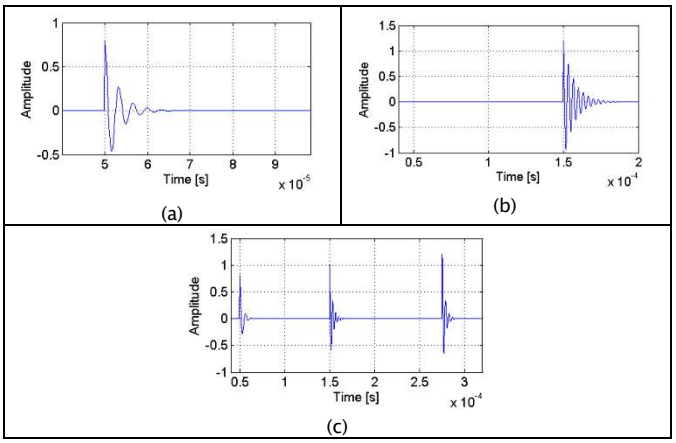

Figure 2. Waveform signals (a) PD1, (b) PD2, (c) PD3
Source: authors

In this work, the PD single-pulse and PD pulse sequence were simulated with a sampling period of $T_s = 0.2\ [\mu s]$. The initial time of PD1 and PD3 is $49.8\ [\mu s]$ and for PD2 is $149.8\ [\mu s]$. The end time of each signal changes. Thus, for PD1 the end time was 99.8 $[\mu s]$, for PD2 was 199.8 $[\mu s]$ and for PD3 was 319.8 $[\mu s]$.

Analysis in time and frequency domain

Analysis in time-domain

In order to obtain the features of PD signals in time-domain a routine in MATLAB © was implemented. This application estimate the peak value (PV), secondary peaks (SP), duration (T) and zero crossing time (ZC) of the PD signals. Table 2 shows the characteristics of PD1 and PD2 single-pulse signals. Comparing the characteristics of PD1 with PD2 it can be observed that both signals have the same frequency (300 kHz) and the zero crossing time is $1 \times 10^{-6}\ [s]$. However, PD1 has fewer secondary peaks than PD2 because the damping factor (τ) of PD1 is also less.

Table 2 Characteristics of PD1 and PD2 signals

Characteristics / Signal	*PD1*	*PD2*
Peak value [p.u.]	0.8	1.2
Peak value time $[\mu s]$	50	150
Zero crossing time $[\mu s]$	50.8	150.8
Secondary peaks	7	12
Duration of signal $[\mu s]$	13	21.2

Source: authors

Characteristics for each pulse that composes the pulse-train PD3 are shown in the Table 3. In this signal, t is constant and the oscillation frequency changes for each pulse (see Table 1). It can be observed that when the frequency of the pulse-train increases the duration and secondary peaks increase too, whereas the zero crossing time decrease.

Table 3 Characteristics of PD3 signal

Characteristics	*Pulse PD3-1*	*Pulse PD3-2*	*Pulse PD3-3*
Frequency (kHz)	150	300	260
Peak value [p.u]	0.8	1	1.2
Peak value time [μs]	50	150	275
Zero crossing time [μs]	51.6	150.8	276
Secondary peaks	2	5	4
Duration [μs]	8,8	9,6	9

Source: authors

Analysis in frequency-domain

The traditional method to analyze signals in frequency domain is the Fourier transform (FT). Figure 3 shows the amplitude of spectrograms for PD1 and PD2. These spectral components are obtained using the Fast Fourier Transformation (FFT), function included in MATLAB©. Analyzing the spectral components of PD single-pulses, the frequency range in which the spectrogram is above 50% of its peak value is from 215 kHz to 410 kHz for PD1 signal and 259 kHz-347 kHz for PD2 signal. However, for both DP signals the peak value of spectrogram is presented at 300 kHz.

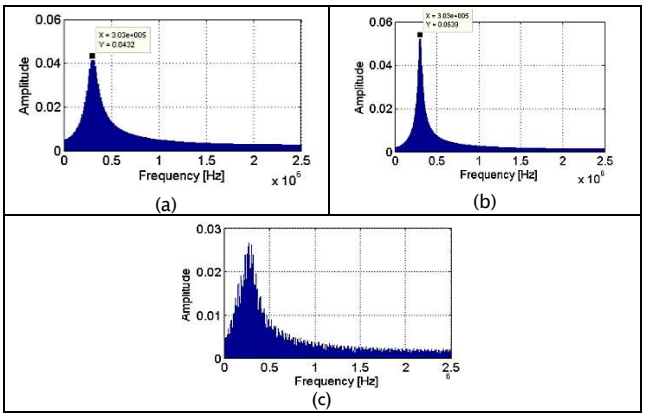

Figure 3. Spectrogram for (a) PD1, (b) PD2, (c) PD3
Source: authors

Figure 3 (c) shows the spectrogram for PD3 signal. It is possible to observe that part of the sequence-pulse frequency is distributed between 130 kHz and 600 kHz, but the frequency of each pulse cannot be identified. For this reason, the spectrogram of each single-pulse is shown in Figure 4.

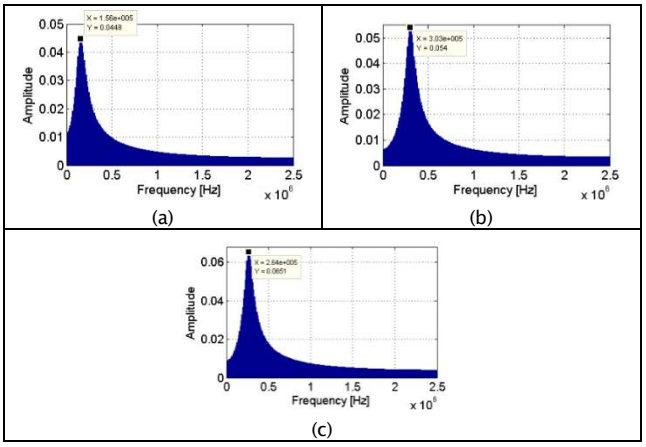

Figure 4. Individual spectrogram for each pulse on PD3 signal (a) pulse PD3-1, (b) pulse PD3-2, (c) pulse PD3-3
Source: authors

It can be observed that peak value of spectrogram for pulse PD3-1, pulse PD3-2 and pulse PD3-3 are presented near to 150 kHz, 300 kHz and 260 KHz, respectively.

Analysis in time-frequency domain

Time-frequency analysis using STFT

In this section the frequency spectra in the time-frequency plane of PD1, PD2 and PD3 are presented. All spectrograms are obtained using a computational application developed by authors. In the first case, STFT was calculated using the LPFT and LPP definitions presented in (4) and (7) with $m = 1$. In all cases, a Gaussian windowing function is used with a bandwidth $h = 250$ samples (duration a 50 μs).

Figure 5 and Figure 6 show the normalized periodogram in two dimensions (2D) for PD1 and PD2 signals, respectively. The predominant energy of PD1 is presented between 240 kHz and 400 kHz at 48 μs-65 μs. On the other hand, for PD2 the frequency is distributed mainly in a range of 230-400 kHz with a time interval of 149.8 μs-160 μs. In both cases the peak value of the periodogram is presented in 300 kHz.

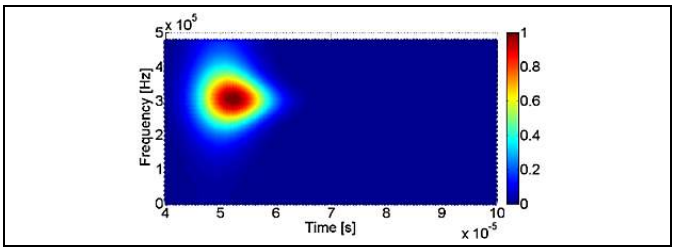

Figure 5. STFT spectrum of PD1 with $\boldsymbol{h = 250}$
Source: authors

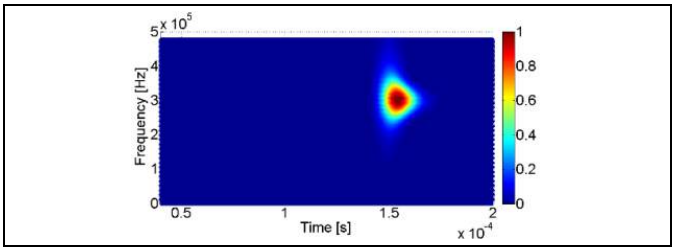

Figure 6. STFT spectrum of PD2 with $\boldsymbol{h = 250}$
Source: authors

Figure 7 shows the spectrum of the PD3 pulse-sequence signal. For PD3-1 pulse the frequency range is between 100 kHz and 200 kHz with a duration of 23 μs (between 40 μs and 63 μs). The periodogram of PD3-2 pulse presents a frequency range of 230-410 kHz in a time interval of 149.8 μs-163 μs. In addition, for the third pulse, the periodogram is located between 274 μs and 288 μs with a frequency range of 180 kHz-400 kHz and a peak value of 260 kHz. Finally, the maximum energy concentration of PD3 sequence-pulse signal is presented in PD3-3, which is the single-pulse that has the highest amplitude of the pulse sequence.

From this time-frequency analysis, it can be concluded that STFT allows to know the relation between time-frequency. However, it not possible to observe low frequency components and the

frequency behavior of signal due to oscillations and ripples related to damping factor. For this reason, this work proposes a time-frequency analysis using LPFT.

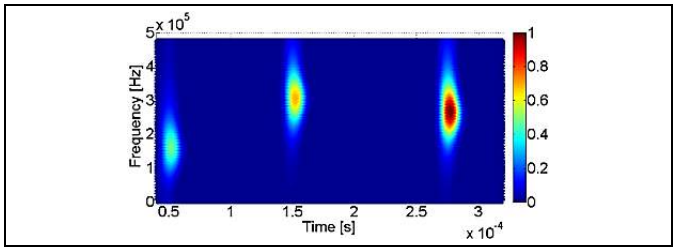

Figure 7. STFT spectrum of PD3 with $\boldsymbol{h = 250}$
Source: authors

Time–frequency analysis using LPFT

In order to promote the advantages and versatility of LPFT, this section presents the analysis of the PD signals using this technique. To estimate LPFT and LPP, definitions in (4) and (7) are applied. However, in this case the polynomial orders were $m = 2$ and $m = 3$. These polynomial orders were selected to reduce the computational complexity, because when m increases the number of operations also increase (Li et al., 2011)

Figure 8 shows the normalized LPP (LPPn) of DP1 signal in 2D. For this PD pulse the LPPn reveals an energy concentration from low frequencies up to 500 kHz. Using both polynomial orders, the peak value of normalized LPP was observed in 300 kHz and located between 51 μs and 56 μs. In addition, LPP shows some lines from low frequency to 250 kHz between 51 and 60 μs. These lines represent the frequency components of the seven secondary peaks (positive and negative) which compose the signal.

It is important to highlight that the energy concentration of the components of low and medium frequency is reduced when signal amplitude decreases. However, when $m = 3$ it is possible to observe that the energy concentration of secondary peaks is increased with respect to the LPP obtained with $m = 2$. In this case, when polynomial order is higher the energy of the signal presents better resolution between 50 and 60 μs.

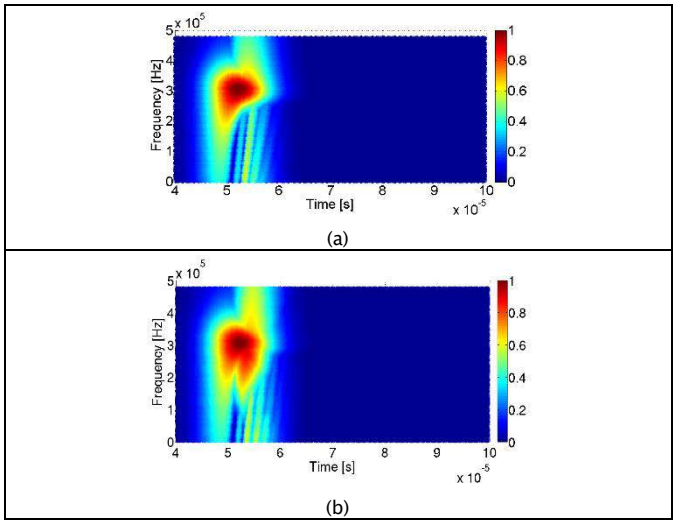

Figure 8. LPP of PD1 with $\boldsymbol{h = 250}$ (a) for $\boldsymbol{m = 2}$ (b) for $\boldsymbol{m = 3}$
Source: authors

The LPPn for PD2 signal is shown in Figure 9. It can be observed that the maximum value of LPP is in 300 kHz at 151[μs]. The energy concentration of DP2 increase from low frequency regions to the maximum value and then decrease. As in PD1 single-pulse, the LPP of PD2 signal shows several lines from low frequency to 300 kHz between 151 μs and 160 μs. These lines are closer to each other due to PD2 pulse varies much faster in time than PD1 signal. Using a polynomial order $m = 3$, the LPP presents a better energy concentration. Furthermore, the frequency spectrum of PD2 signal obtained with a third order LPFT presents components of low and medium frequency (vertical lines between 151 μs-160 μs) with higher energy than those observed in the LPP when $m = 2$.

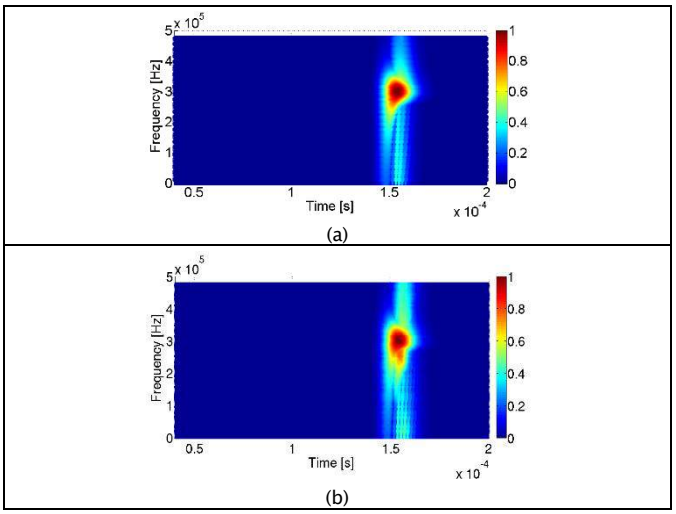

Figure 9. LPP of PD2 with $\boldsymbol{h = 250}$ (a) for $\boldsymbol{m = 2}$ (b) for $\boldsymbol{m = 3}$
Source: authors

Figure 10 shows the LPPn of PD3 pulse-sequence signal. For the three pulses PD3-1, PD3-2 and PD3-3 the LPPn reveals an energy concentration from low frequencies up to 150 kHz, 300 kHz and 260 kHz, respectively. In the case of PD3-1, the frequency range of highest energy concentration is between 120 kHz and 180 kHz with duration of 20 μs (between 40 μs and 60 μs). For PD3-2 the highest energy concentration presents a frequency range of 250-350 kHz in a time interval of 149.8 μs-158 μs. Finally, for third pulse, the highest energy concentration of LPP is located between 264 μs and 280 μs with a frequency range of 200 kHz-300 kHz and a peak value of 260 kHz.

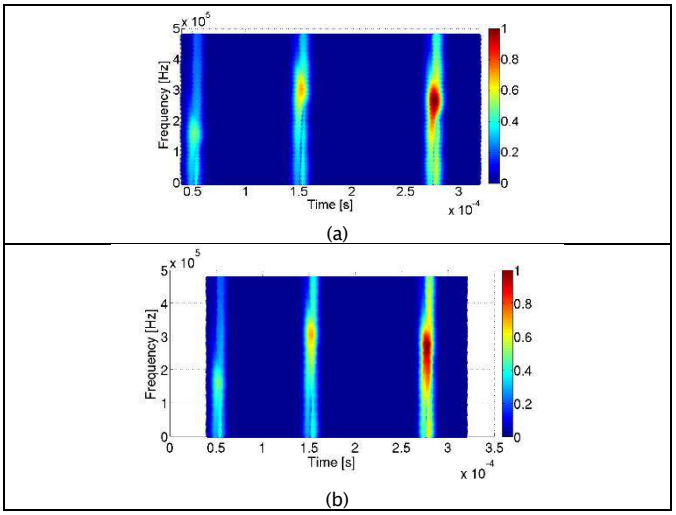

Figure 10. LPP of PD3 with $\boldsymbol{h = 250}$ (a) for $\boldsymbol{m = 2}$ (b) for $\boldsymbol{m = 3}$
Source: authors

Manner similar to the spectrum obtained for single-pulse signals, Figure 10 shows some lines related with low and medium frequency components. These components have frequencies from 200 Hz to the frequency where the LPP is maximum (for three pulses). These lines represent the frequency components of secondary peaks and fluctuations, which compose each pulse. When secondary peaks increase, these components increase too. The energy concentration of these additional components depend on the peak value. Finally, the maximum energy concentration of PD3 signal is presented in PD3-3, which is the single-pulse that has the highest amplitude of the pulse sequence.

Conclusions

In this paper, the process to use local polynomial Fourier transform (LPFT) for analysis of partial discharge pulses was described. This signal processing technique is presented as an effective method in the time-frequency domain to study electrical transient signals. For PD signals this analysis took into account their amplitude, duration, secondary peaks, frequency components and energy concentration.

Main frequency components of the PD pulses in the time-frequency plane can be correctly obtained by STFT and LPFT. However, the LPP provided by the LPFT allows to observe low and medium frequency components (from 200 Hz to maximum frequency of signal) related with the secondary peaks and fluctuations of the DP pulses, which are not detected when the STFT is used. In addition, the LPFT provides the highest energy concentration of PD sequence-pulses.

Finally, simulations show that the LPP of the analyzed PD signals presents a better resolution (in time and frequency) when the polynomial order is $m = 3$. Using this polynomial order the energy concentration of the secondary peaks is increased and the frequency components of the damping oscillatory portion of the PD signal are easier to identify.

References

Caironi, C., Brie, D., Durantay, L., Rezzoug, A., Champigneulles, R., Nancy, U. H. P., … Vandoeuvre, L. (2002). Interest & utility of time frequency and time scale transforms in the partial discharges analysis. In *IEEE International Symposium on Electrical Insulation* (pp. 516–522).

Chai, M. L., Md Thayoob, Y. H., Ghosh, P. S., Sha'ameri, A. Z., & Talib, M. A. (2006). Identification of different types of partial discharge sources from acoustic emission signals in the time-frequency representation. In *Proceedings First International Power and Energy Conference (PECon 2006),* (pp. 580–585).

Katkovnik, V. (1995). A new form of the Fourier transform for time-varying frequency estimation. *Signal Processing*, *47*, 187–200.

Katkovnik, V. (1997). Nonparametric Estimation of Instantaneous brequency, *Statistics & Probability Letters*. *43*(1), 183–189.

Li, X., & Bi, G. (2009). The reassigned local polynomial periodogram and its properties. *Signal Processing*, *89*(2), 206–217.

Li, X., Bi, G., Stankovic, S., & Zoubir, A. M. (2011). Local polynomial Fourier transform: A review on recent developments and applications. *Signal Processing*, *91*(6), 1370–1393.

Lu, Y., & Boxue, D. (2008). Eperimental Study on Pattern Identification of Transformer Partial Discharge by Filtering Method Matching Time and Frequency. *ELECTRIC POWER*, *41*, 16–19.

Ma, X., Zhou, C., & Kemp, I. J. (2002). Interpretation of wavelet analysis and its application in partial discharge detection. *IEEE Transactions on Dielectrics and Electrical Insulation*, *9*, 446–457.

Mortazavi, S. H., & Shahrtash, S. M. (2008). Comparing denoising performance of DWT,WPT, SWT and DT-CWT for Partial Discharge signals. In *2008 43rd International Universities Power Engineering Conference* (pp. 1–6). IEEE.

Phukan, R., & Karmakar, S. (2000). Acoustic Partial Discharge Signal Analysis using Digital Signal Processing Techniques. In *IEE Indian Conference (INDICON)* (pp. 1–6).

Popović, V., Djurović, I., Stanković, Lj., Thayaparan, T., & Daković, M. (2010). Autofocusing of SAR images based on parameters estimated from the PHAF. *Signal Processing*, *90*, 1382–1391.

Sejdić, E., Djurović, I., & Jiang, J. (2009). Time–frequency feature representation using energy concentration: An overview of recent advances. *Digital Signal Processing*, *19*(1), 153–183.

Stanković, Lj., & Djukanović, S. (2005). Order adaptive local polynomial FT based interference rejection in spread spectrum communication systems. *IEEE Transactions on Instrumentation and Measurement*, *54*(6), 2156–2162.

Sun, C., Wang, B., Fang, Y., Yang, K., & Song, Z. (2015). High-resolution ISAR imaging of maneuvering targets based on sparse reconstruction. *Signal Processing*, *108*, 535–548.

Thayaparan, T., Djurovic, I., & Stankovic, L. (2006). Focusing distorted ISAR images using Adaptive Local Polynomial Fourier Transform. *2006 International Radar Symposium*, *1*(2), 2–5.